Supplementary Materials

Construction of triazine/heptazine carbon nitride homojunction for photocatalytic reduction of high-concentration 4-nitrophenol

Haojie Tong, Jingyu Zhang, Wendi Wang, Lanhao Yang, Zhiyi Zhang, Qiyue Jia, Zhanli Chai*, Kun Lan*

College of Energy Materials and Chemistry, College of Chemistry and Chemical Engineering, Inner Mongolia Key Laboratory of Rare Earth Catalysis, Inner Mongolia University, Hohhot 010021, Inner Mongolia, China.

***Correspondence to:** Prof. Kun Lan, Prof. Zhanli Chai, College of Energy Materials and Chemistry, College of Chemistry and Chemical Engineering, Inner Mongolia University, Hohhot 010021, Inner Mongolia, China. E-mail: k_lan@imu.edu.cn; chaizhanli@imu.edu.cn

Theoretical details:

The theoretical calculation part was completed by the CASTEP code using ultrasoft pseudopotential. The geometric optimization process used the Perdew-Burke-Ernzerh equation originating from generalized gradient approximation (GGA). The convergence criterion for energy and force are $1.0*e^{-5}$ eV/atom and 0.03 eV/A. The Grimme method was adopted to describe the van der Waals interaction63. Cut-off energy and the value of K-point mesh were determined to be 500 eV, and 3*3*1 after convergence tests. The slab models of TCN and HCN were obtained by cleaving (002) crystal planes of bulk TCN and bulk HCN. The monolayer slab model of TCN and the monolayer slab model of HCN are geometrically optimized accompanied by a vacuum layer thickness of 15 Å. The information on the work function is then obtained by property calculations. The crystallized carbon nitride homojunction model was constructed using a monolayer slab of TCN and a monolayer slab of HCN crystalline surfaces and the lattice mismatch was within 5%. The vacuum layer thickness of the homojunction model is set to 20 Å. The optimized structural parameters for the homojunction model are as follows, a = b = 8.0234 Å, c = 25.1154 Å. Light irradiation conditions were simulated by an applied electric field in the z-direction[1].

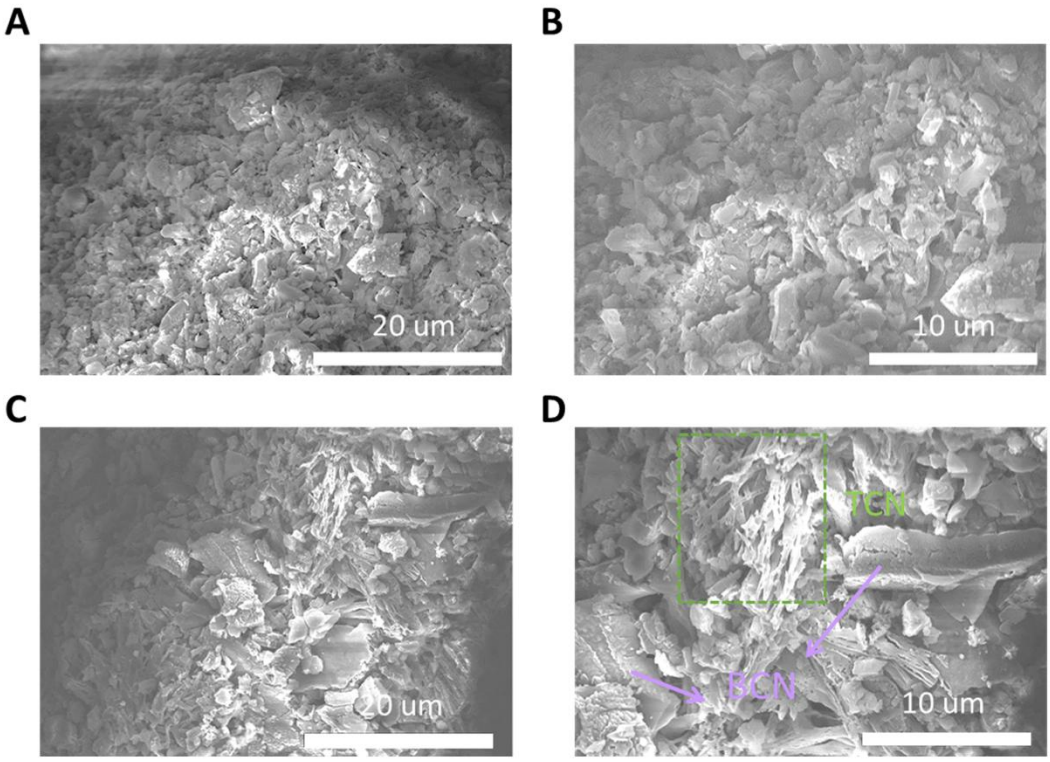

Supplementary Figure 1. (A and B) SEM images of BCN (bulk phenazine-based C_3N_4 after calcined melamine at 500 ℃ for 4 h); (C and D) SEM images of HCN (homojunction carbon nitride after calcined melamine at 500 ℃ for 2 h).

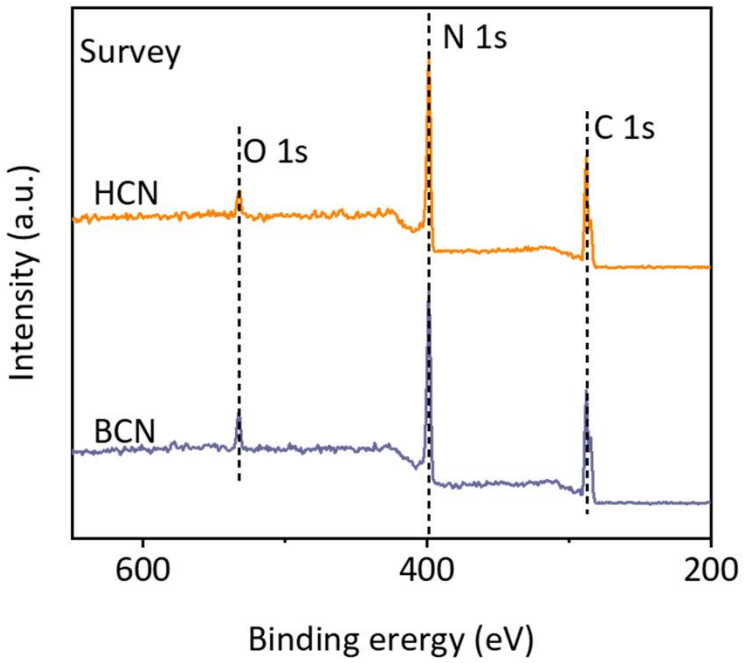

Supplementary Figure 2. The XPS survey spectra of HCN (homojunction carbon nitride after calcined melamine at 500 ℃ for 2 h) and BCN (bulk phenazine-based C_3N_4 after calcined melamine at 500 ℃ for 4 h).

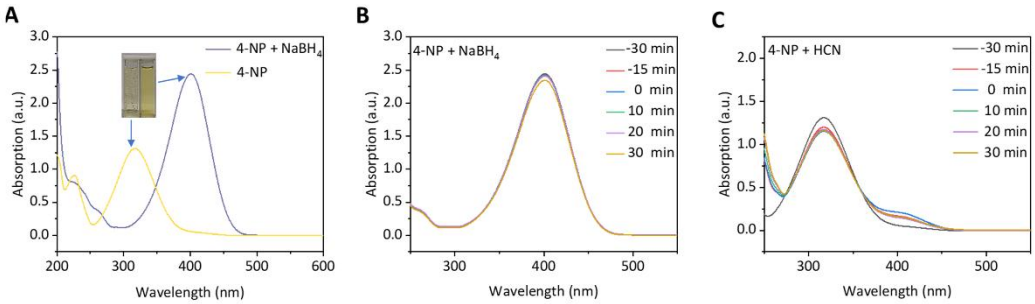

Supplementary Figure 3. (A) Comparison of UV-vis spectra before and after the addition of $NaBH_4$; (B) Comparison of UV-vis spectra at different time intervals after adding $NaBH_4$; (C) Comparison of UV-vis spectra at different time intervals after addition of HCN (homojunction carbon nitride after calcined melamine at 500 ℃ for 2 h).

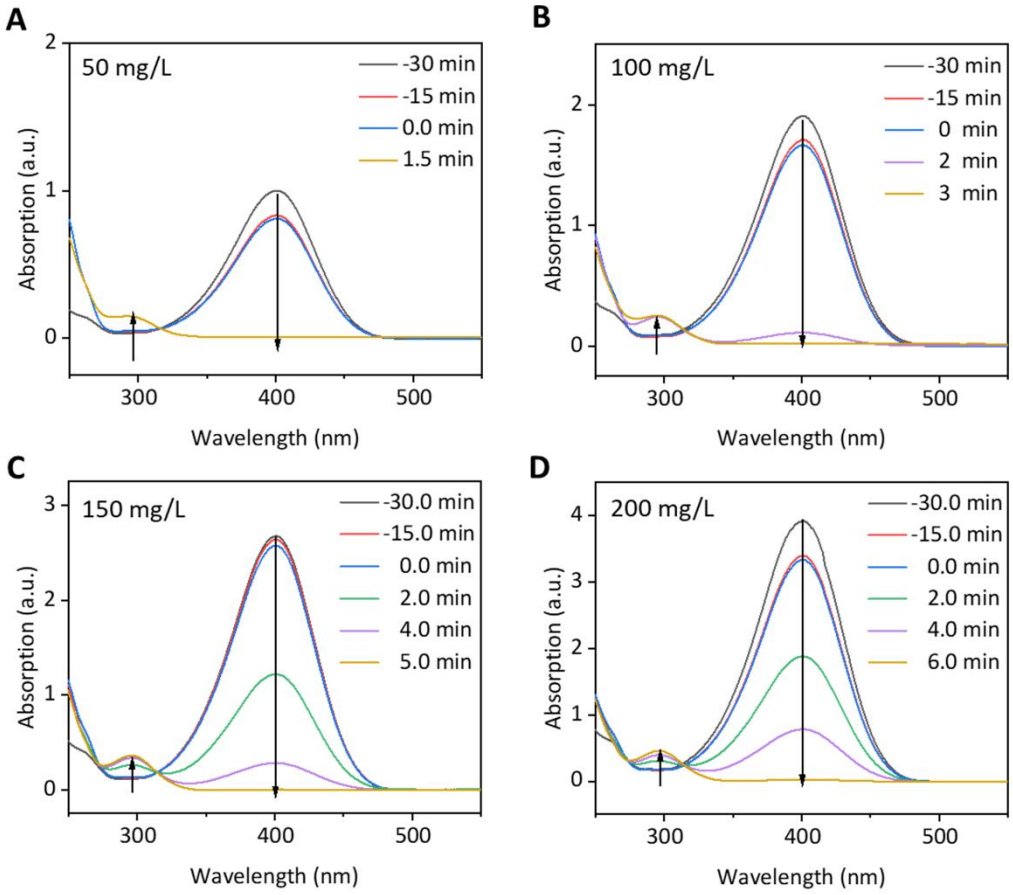

Supplementary Figure 4. UV-vis absorption spectra for different concentrations of 4-NP reduction with 5.0 mg of HCN under visible light irradiation: (A) 50 mg/L, (B) 100 mg/L, (C) 150 mg/L, (D) 200 mg/L.

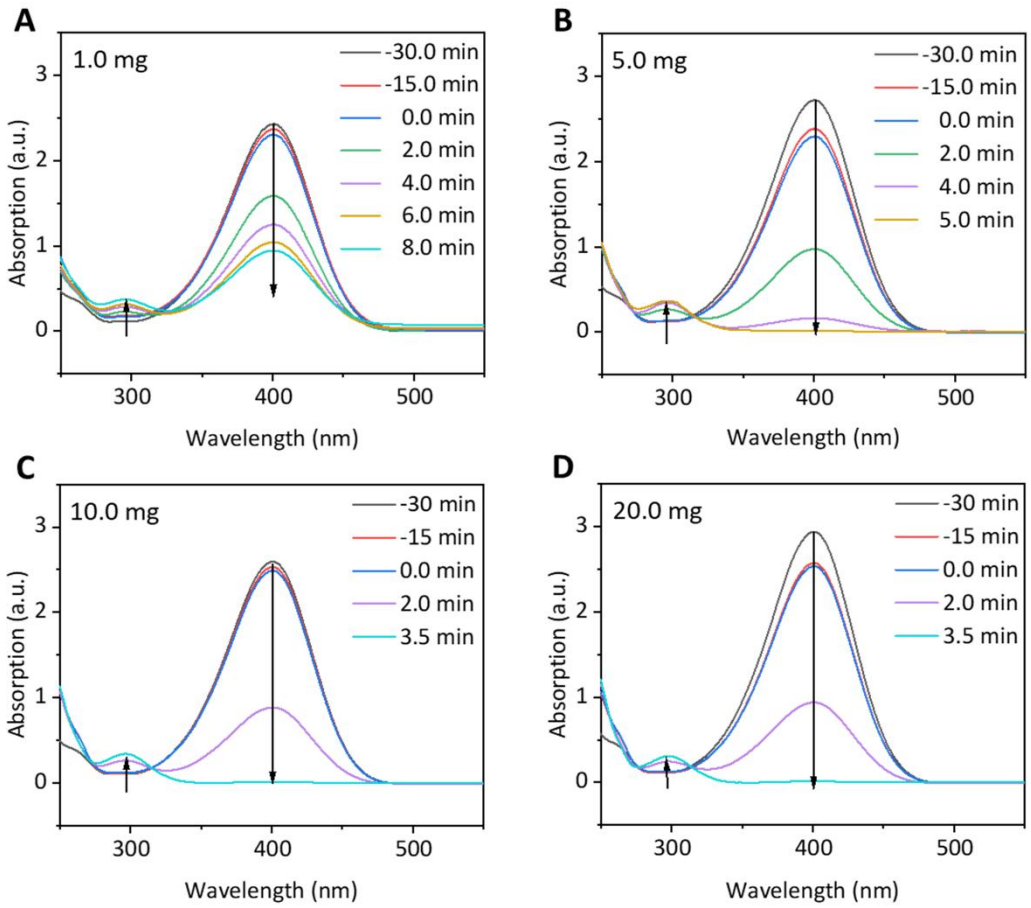

Supplementary Figure 5. UV-vis absorption spectra for 150 mg/L 4-NP reduction with different amounts of HCN under visible light irradiation: (A) 1.0 mg, (B) 5.0 mg, (C) 10.0 mg, (D) 20.0 mg.

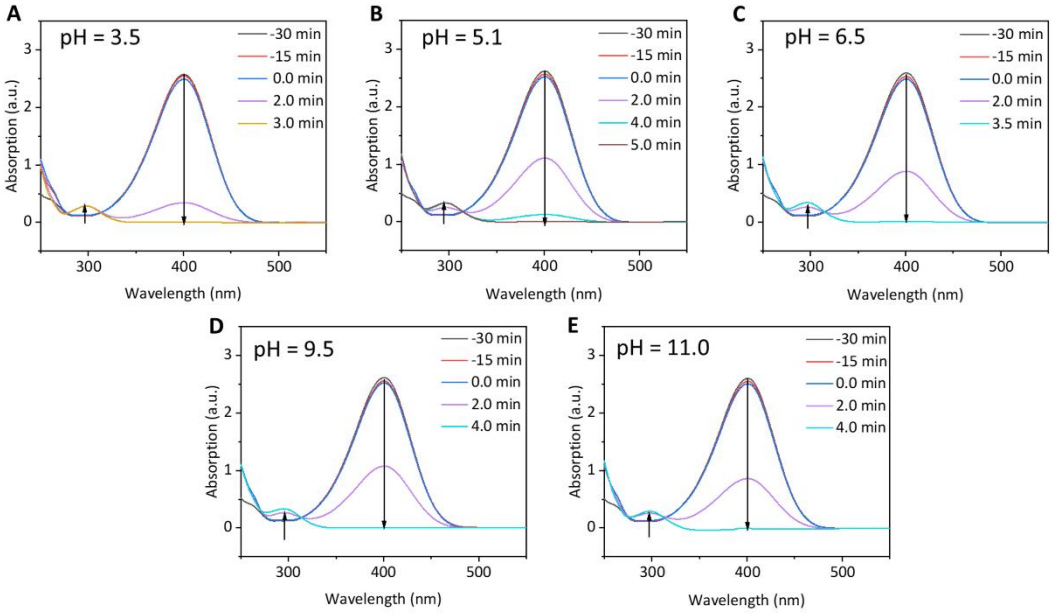

Supplementary Figure 6. UV-vis absorption spectra for 150 mg/L 4-NP reduction with 10.0 mg of HCN in different pH under visible light irradiation: (A) pH = 3.5, (B) pH = 5.1, (C) pH = 6.5, (D) pH = 9.5, (E) pH = 11.0.

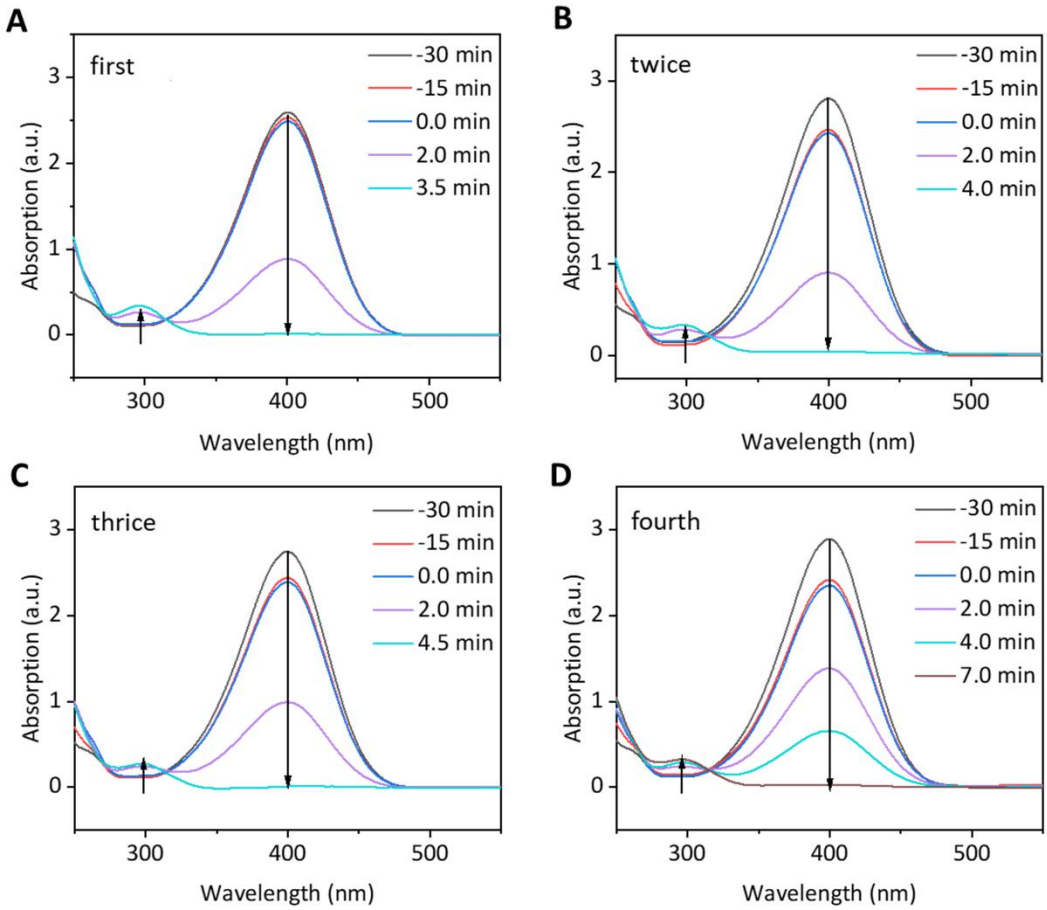

Supplementary Figure 7. UV-vis absorption spectra for 150 mg/L 4-NP reduction with 10.0 mg of HCN after 4 times recyclability under visible light irradiation: (A) first, (B) twice, (C) thrice, (D) fourth.

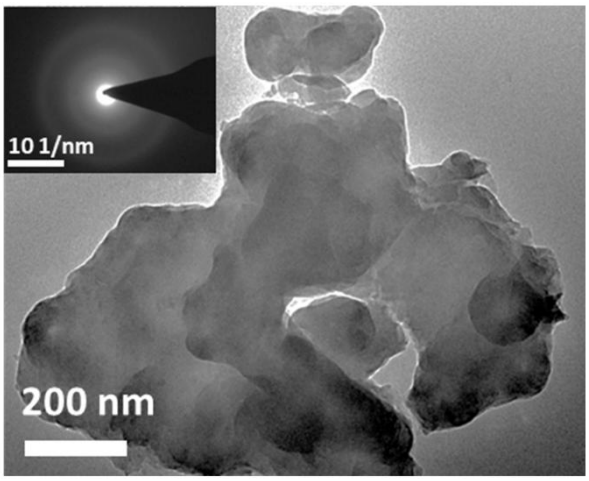

Supplementary Figure 8. TEM image of the cycled HCN (homojunction carbon nitride after calcined melamine at 500 ℃ for 2 h).

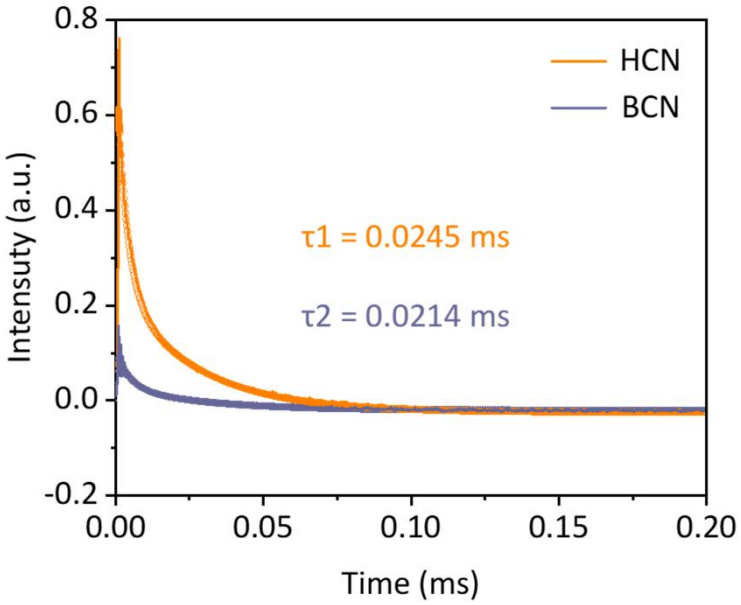

Supplementary Figure 9. TPV curves and charge attenuation time of HCN (homojunction carbon nitride after calcined melamine at 500 ℃ for 2 h) and BCN (bulk phenazine-based C_3N_4 after calcined melamine at 500 ℃ for 4 h).

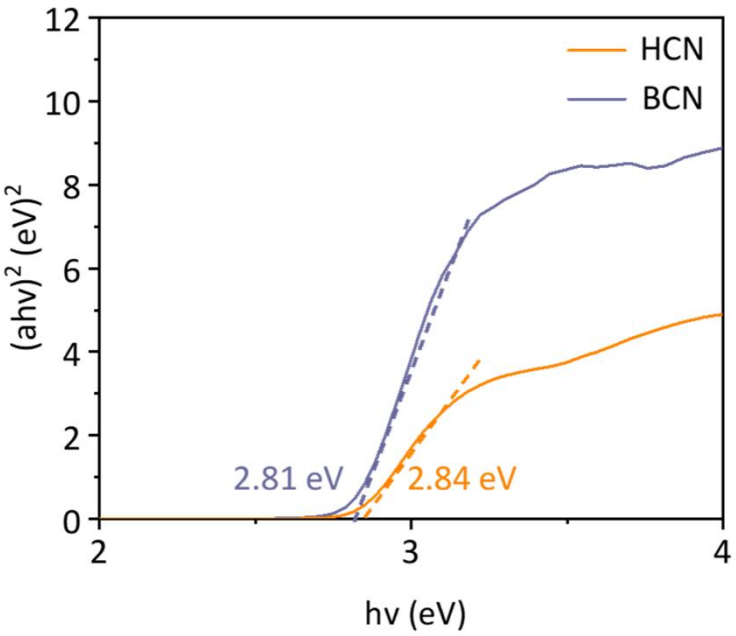

Supplementary Figure 10. Taut plots for band gap determination of HCN (homojunction carbon nitride after calcined melamine at 500 ℃ for 2 h) and BCN (bulk phenazine-based C_3N_4 () after calcined melamine at 500 ℃ for 4 h).

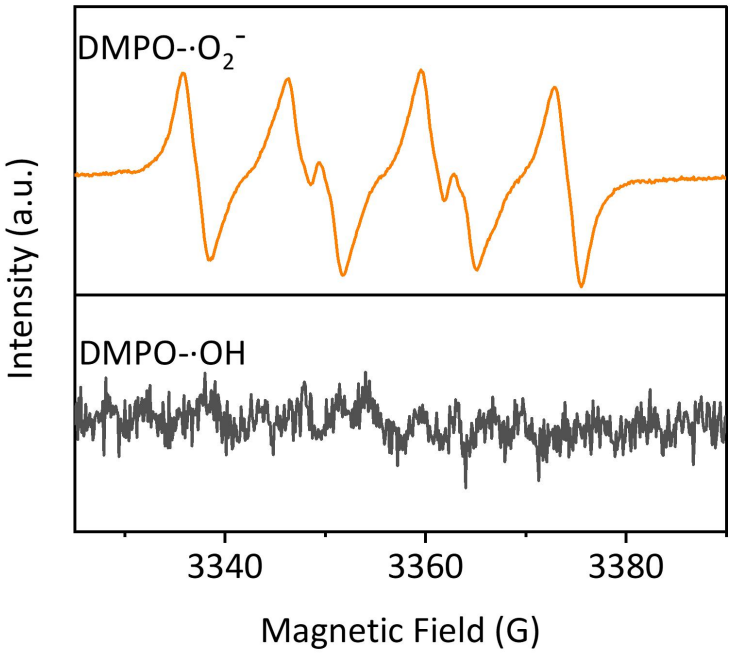

Supplementary Figure 11. EPR detection of DMPO-·O_2^- and DMPO-·OH species during calcined melamine at 500 ℃ for 2 h using HCN (homojunction carbon nitride) under visible light irradiation for 10 min.

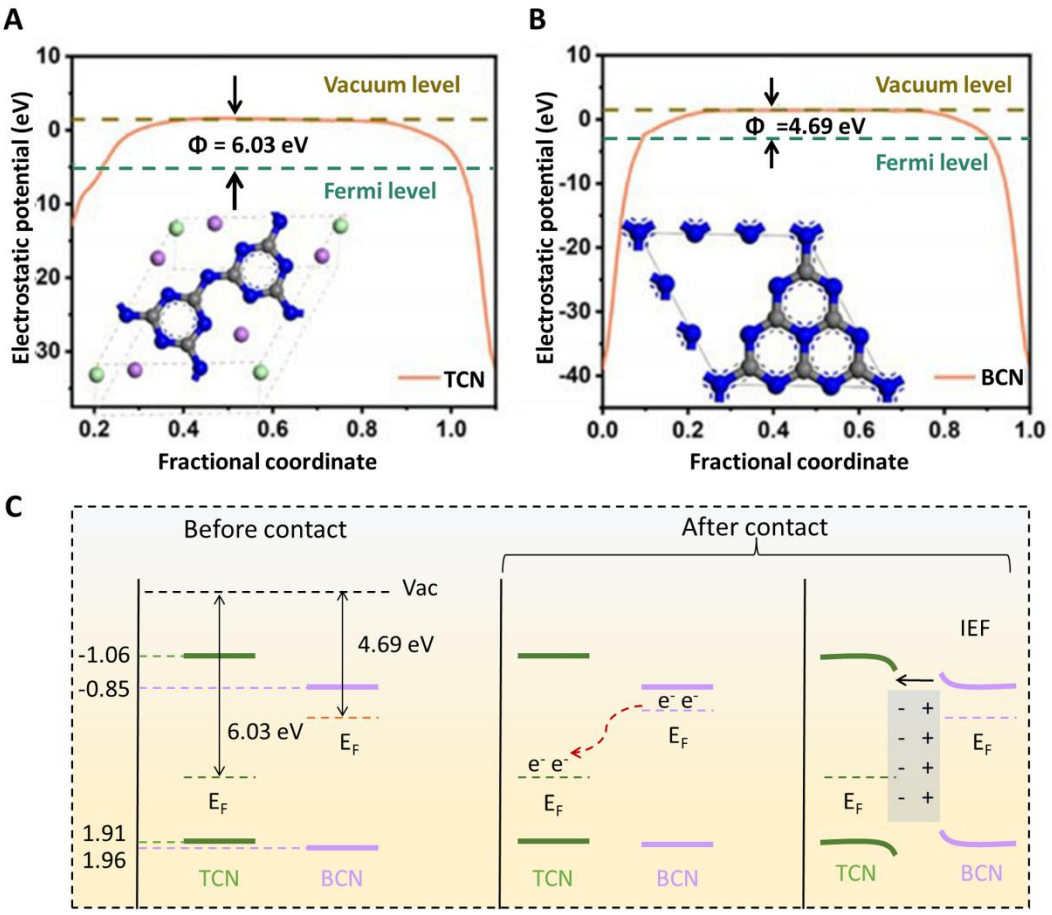

Supplementary Figure 12. Work functions for (A) TCN and (B) BCN, and the insets show the top view of the corresponding slab models. (C) The schematic illustration of the electron transfer mechanism under a dark environment. Color scheme: N, blue; C, gray; Cl^-, green; and, Li^+, pink.

Supplementary Table 1. Comparison of apparent rate constants (*k*) of different photocatalysts under visible light irradiation

Catalyst	4-NP concentration (mg/L)	Light source	Reducer	Reaction time (min)	*k* (min^{-1})	Ref.
CdS-0.03(MoS_2-0.01rGO)	20	500 W Xe lamp	$HCOONH_4$	18	0.084	[2]
NrGo/g-g PSCN	15	250 W Hg lamp	No	180	0.024	[3]
N-GQDs	140	NIR light	$NaBH_4$	8	0.704	[4]
M@A-16%	20	NO	$NaBH_4$	25	0.101	[5]
TNOS-1-Ag16	20	300 W Xe lamp	$NaBH_4$	12	0.828	[6]
TNOS-1-Au8	20	300 W Xe lamp	$NaBH_4$	4	1.165	[6]
Pd NSs/CNNSs	20	No	$NaBH_4$	6	0.760	[7]
ZnCdSe/CuS	10	250 W Xe lamp	$NaBH_4$	120	0.014	[8]
DCM-TPA-Pt	1	250 W Xe lamp	$NaBH_4$	3	1.83	[9]
TiO_2/CdS	1	365 nm UV light	$NaBH_4$	20	0.1269	[10]
BCN	100	400 W Xe lamp	$NaBH_4$	9	0.630	**This work**
HCN	100	400 W Xe lamp	$NaBH_4$	3.5	1.440	**This work**

Supplementary Table 2. Apparent rate constants (*k*) for photocatalytic reduction of 4-NP with HCN under visible light at different concentrations, catalyst amounts, and different pH values

Different conditions		***k*** **(min^{-1})**
c (4-NP)/mg·L^{-1}	50	2.84
	100	1.38
	150	1.20
	200	0.75
m (HCN)/mg	1.0	0.11
	5.0	1.23
	10.0	1.49
	20.0	1.35
pH (4-NP)	3.5	1.72
	5.1	1.02
	6.5	1.49
	9.5	1.24
	11.0	1.23

REFERENCES

1. Li F, Yue X, Liao Y, Qiao L, Lv K, Xiang Q. Understanding the unique S-scheme charge migration in triazine/heptazine crystalline carbon nitride homojunction. *Nat Commun* 2023; 14: 3901-11. DOI: 10.1038/s41467-023-39578-z.
2. Peng W, Chen Y, Li X. MoS_2/reduced graphene oxide hybrid with CdS nanoparticles as a visible light-driven photocatalyst for the reduction of 4-nitrophenol. *J Hazard* 2016; 309: 173-9. DOI: 10.1016/j.jhazmat.2016.02.021.
3. Padhiari S, Tripathy M, Hota G. Nitrogen-doped reduced graphene oxide covalently coupled with graphitic carbon nitride/sulfur-doped graphitic carbon nitride heterojunction nanocatalysts for photoreduction and degradation of 4-nitrophenol. *ACS Appl Nano Mater* 2021; 4: 7145-61. DOI: 10.1021/acsanm.1c01126.
4. Liu H, Wang H, Qian Y, et al. Nitrogen-doped graphene quantum dots as metal-free photocatalysts for near-infrared enhanced reduction of 4-nitrophenol. *ACS Appl Nano Mater* 2019; 2: 7043-50. DOI: 10.1021/acsanm.9b01549.
5. Qin X, Ding C, Tian Y, Dong J, Cheng B. Multifunctional $Ti_3C_2T_x$ MXene/silver nanowire membranes with excellent catalytic, antifouling, and antibacterial properties for nitrophenol-containing water purification. *ACS Appl Mater Inter* 2023; 15: 48154-67. DOI: 10.1021/acsami.3c09983.
6. Wu J, Wang J, Wang T, et al. Photocatalytic reduction of p-nitrophenol over plasmonic M (M = Ag, Au)/$SnNb_2O_6$ nanosheets. *Appl Surf Sci* 2019; 466: 342-51. DOI: 10.1016/j.apsusc.2018.09.222.
7. Gu K, Pan X, Wang W, et al. In situ growth of Pd nanosheets on g-C_3N_4 nanosheets with well-contacted interface and enhanced catalytic performance for 4-nitrophenol reduction. *Small* 2018; 14: 1801812-20. DOI: 10.1002/smll.201801812.
8. Sahu J, Mishra BP, Parida K. $Zn_{0.5}Cd_{0.5}Se$ embedded CuS 0D/2D S-scheme heterojunction for surface-plasmon-resonance enhanced photocatalytic H_2O_2 production and para-nitrophenol reduction. *ACS Appl Energy Mater* 2024; 8: 388-402. DOI: 10.1021/acsaem.4c02494.
9. Zhou S, Luo X, Zhang Y, et al. Quaternization of a triphenylamine-based conjugated porous organic polymer to immobilize $PtCl_6^{2-}$ for the photocatalytic reduction of 4-nitrophenol. *Inorg Chem* 2024; 63: 15024-33. DOI: 10.1021/acs.inorgchem.4c01789.
10. Singh N, Mondal K, Misra M, Sharma A, Gupta RK. Quantum dot sensitized electrospun mesoporous titanium dioxide hollow nanofibers for photocatalytic applications. *RSC Adv* 2016; 6: 48109-19. DOI: 10.1039/c6ra04305d.